applied microbiology

Communication

Nile Tilapia Skin Impregnated with Antibacterial Silver/Titanium Dioxide Compounds

Maíra Cristina Marcolino [1], Milena Lima Guimarães [1], Jorge Alexandre Alencar Fotius [1], Leda Maria Saragiotto Colpini [2], Mateus Matiuzzi da Costa [1] and Helinando Pequeno de Oliveira [1,*]

[1] Institute of Materials Science, Federal University of São Francisco Valley, Avenida Antônio Carlos Magalhães, 510-Santo Antônio, Juazeiro 48902-300, CEP, Brazil
[2] Curso Superior de Tecnologia em Biocombustíveis, Setor Palotina, Federal University of Parana, Rua Pioneiro 2153, Jardim Dallas, Palotina 85950-000, CEP, Brazil
* Correspondence: helinando.oliveira@univasf.edu.br

Abstract: The development of alternative (and free-of-antibiotics) antibacterial and antibiofilm agents is an important strategy to circumvent the resistance of bacteria to antibiotics. Herein, we explore the production of mixed oxides by incorporating silver nanoparticles in titanium dioxide as a silver concentration-dependent antibacterial agent that is further incorporated in Tilapia fish skin (a promising prototype of xenograft), integrating the antibacterial activity of mixed oxide into the intrinsic properties of Tilapia skin. The antibiofilm activity of samples prepared with high concentrations of silver (10 wt% of precursor $AgNO_3$) has been considered a good antibiofilm response. The influence of silver content is also observed with respect to the minimum bactericidal concentration, which is reduced to 3.13 mg/mL with a characteristic kill time in the order of 30 min that is associated with antibiofilm activity in biofilm-forming strains of *Staphylococcus aureus*. These results indicate that modified Tilapia fish skin acquires antibacterial behavior and can be explored for xenografts with prospective applications in the light-dependent actuation of TiO_2-based compounds.

Keywords: nanomaterials; silver nanoparticles; mixed oxide; xenograft; antibiofilm; *S. aureus*

check for updates

Citation: Marcolino, M.C.; Guimarães, M.L.; Fotius, J.A.A.; Colpini, L.M.S.; da Costa, M.M.; de Oliveira, H.P. Nile Tilapia Skin Impregnated with Antibacterial Silver/Titanium Dioxide Compounds. *Appl. Microbiol.* **2023**, *3*, 265–275. https://doi.org/10.3390/applmicrobiol3010018

Academic Editor: Seung-Chun Park

Received: 26 January 2023
Revised: 3 February 2023
Accepted: 8 February 2023
Published: 10 February 2023

1. Introduction

New sensors and smart devices are now possible via the burgeoning growth of nanotechnology that makes use of building blocks with outstanding properties such as large surface areas and multifunctional properties, with relevant applications in antibacterial products [1,2]. The different forms of silver (Ag^0, Ag_2O, and Ag^+) have been extensively reported in the literature as important antibacterial agents [3–5] due to their intrinsic ability to be accumulated in microorganisms affecting vital processes.

The accumulation of silver nanostructures on the cell wall favors cell disruption (damage in the cell envelope) [6,7] with respect to the subsequent release of Ag^0 and Ag^+ species, which are characterized by a strong affinity toward sulfur proteins (interaction with thiol groups (-SH) and phosphorous components in DNA) [8,9]. As a consequence, the interruption in adenosine triphosphate production is established, with implications for DNA replication. The binding of these species in the phosphoric acid residues of DNA (the N7 atom of guanine) disturbs replication and cell division [6]. In addition to this mechanism, the creation of reactive oxidative species (ROS) introduces genotoxic effects during the destruction of cells and biofilms [6,8,9].

On the other hand, titanium dioxide has been recognized as an important photoactive support applied in environmental remediation [10–12], considering the prevailing (and stable) rutile and anatase phases [13]. Improvements in the antibacterial activity of TiO_2 are based on the incorporation of metal nanoparticles as doping components [14]. With this aim, acrylic and composite resins [8,15,16], TiO_2/Ag membranes [17], and titanium coatings [8] have been developed for several applications, such as endodontic treatment, dental implant

intervention [8,18], the prevention of oral biofilm formation [19] and superhydrophobic coatings for wood substrates [20].

The incorporation of silver nanoparticles into TiO_2 structures is conducted using different methods, such as chemical vapor deposition, horizontal vapor phase growth, sonochemical methods, ion implantation [5], photochemical methods, radiation, ion/magnetron sputtering [21], sol–gel processes [12,22,23], micro-arc oxidation [24], and plasma electrolytic oxidation [25], which commonly introduces high-energy-requirement issues. An alternative and simple method for the production of titanium dioxide support for the following impregnation and doping steps with silver nanoparticles can be successfully conducted by incipient wetness impregnation (IWI) procedures [26,27] in which the aqueous solution of the metal precursor is incorporated into the support with the resulting fine paste being thermally treated in order to be converted in a mixed oxide of titanium and silver.

An important step to improve the antibacterial activity of the synthesized mixed oxides is the adequate incorporation of material on a scaffold that potentializes its action for wound-dressing applications. Tilapia skin has been progressively applied as a scaffold for treating burns [28,29]. The impregnation of antibacterial components in tilapia skin can be conveniently explored for the sterilization of skin [28] and for avoiding biofilm contamination on surfaces. Previous experiments conducted by our group considered the use of conducting polymers and graphene derivatives as a strategy to incorporate antibacterial properties into the tilapia skin [30]. Relative to the safety of the proposed antimicrobial skin, some aspects must be highlighted: lyophilization removes 95% of the water from the skin, introducing an important impediment to biochemical processes and microbial action [31]. This process favors the use of xenograft substrates [32], with collagen accelerating the healing process [33,34]. The incorporation of mixed oxides (silver nanoparticles immersed in a TiO_2 template) introduces antibacterial properties for the modified skin with the advantages of good biocompatibility with titanium dioxide [35,36], while silver nanoparticles improve the kinetics of antibacterial activity [37], which is associated with preservation of skin collagen [38] and lower toxicity for eukaryotic cells than compared with procaryotic cells [39].

Therefore, a mixed oxide powder of silver and titanium was produced by the IWI method and for use as a prototype of an antibacterial and antibiofilm agent incorporated into the tilapia skin, which produces antibacterial and antibiofilm properties preserving the intrinsic structure of the xenograft support.

2. Materials and Methods

2.1. Materials

Titanium dioxide (Êxodo Científica, São Paulo, Brazil) and silver nitrate (Sigma-Aldrich, São Paulo, Brazil) were used as received. Nile tilapia skins were donated by Omega Pescados do Vale (Petrolina, Pernambuco, Brazil). Deionized water with a resistivity of 18.2 MΩcm was used in all experiments. The phosphate saline solution (PBS) was prepared from a dispersion of 8.2 g of sodium chloride, 1.05 g of sodium phosphate, and 0.355 g of monobasic sodium phosphate in milli-Q water (1 L) at pH 7.2.

2.2. Synthesis of Mixed Oxides

Preceding the synthesis of a mixed oxide of Ag/TiO_2, an initial step of drying TiO_2 was carried out in an oven for 21 h at 120 °C. Dried TiO_2 (30 g) was dissolved in water (30 mL) and acquired the aspect of a fine paste. After this initial step, different ratios of the metal precursor—$AgNO_3$—were prepared (0.9638 g—2 *w*/*w*%; 5.2477 g—10 *w*/*w*%). Then, different amounts of silver nitrate (already dissolved in water—2.4 mL for the sample with 2% of Ag; 12.4 mL for the sample with 10% of Ag) were added to TiO_2 paste. The final solutions were kept under constant rotation (120 rpm) for 17 h in a rotary evaporator (Fisatom, São Paulo, Brazil) at room temperature, with the excess solvent eliminated by additional vacuum evaporation on a rotary evaporator at 80 °C. Then, the material was removed from the flask and dried in an oven for 21 h at 120 °C and then calcined with a

heating ramp at 400 °C for 5 h, resulting in 2% Ag/TiO_2 and 10% Ag/TiO_2 samples that were prepared at increasing concentrations of silver. The negative control was prepared in the absence of silver (sample 0% Ag/TiO_2).

2.3. Tilapia Skin Treatment and Lyophilization

The tilapia skin was previously treated according to Guimarães et al. [30] with some modifications. Scales and excess residual meat were removed with a razor. Then, circular disks of tilapia skin that were 1 cm in diameter were separated and washed with ultrapure water and immersed in a phosphate saline solution (PBS) at 37 °C for 30 min. After the pretreatment, the skins were frozen and then lyophilized following a methodology adapted from Lima et al. [31] and Nie et al. [40]. For this, the skin disks were frozen at −25 °C for a period of 24 h. Then, the skins were lyophilized under a vacuum for 30 min. The resulting material was placed in sterile glass containers and stored at −10 °C and transferred to a laminar flow hood, remaining under ultraviolet radiation for 15 min.

2.4. Impregnation of Mixed Oxides in Tilapia Skin

For the impregnation of mixed oxides in tilapia skin, modifications were incorporated into the procedure reported in Ref. [41]: 100 mg of the previously prepared samples (0% Ag/TiO_2, 2% Ag/TiO_2, and 10% Ag/TiO_2) was dispersed in 1 mL of ultrapure water and kept under sonication for 15 min. The treated disks of tilapia skin were immersed in mixed oxide solutions for impregnation by rehydrating the skin with mixed oxide solutions for 30 min in an ultrasonic bath. After sonication, skins were removed from the solutions and transferred to sterile Petri dishes and taken to a laminar flow hood to dry at room temperature.

2.5. Characterization Techniques

Fourier transform infrared spectroscopy was used to scrutinize the structure of the composite synthesized from the KBr method in a Shimadzu Prestige-21 IR spectrophotometer (Japan) in the range of 4500–450 cm^{-1} (step of 1 cm^{-1}). Scanning electron micrographs were provided by a Vega 3XM Tescan scanning electron microscope (Tescan, Brno, Czechia) at an accelerating voltage of 10 kV with samples previously coated with a thin layer of gold (120 nm). Particle size and the zeta potential were measured on a Zetasizer Nano-ZS90 Malvern particle analyzer. The phase composition was determined by X-ray diffraction analyses. X-ray diffraction (XRD) patterns were performed at room temperature with a Rigaku Miniflex powder diffractometer (Rigaku Corporation, Tokyo, Japan), with Cu-Kα radiation (λ = 1.5418 Å) and with the tube operating at 40 kV and 15 mA in continuous mode with a sweep rate of 0.02° at a speed of 20°/min. The phase composition was determined by the Rietveld method using the FullProof Suite program in association with references from the ICSD database.

2.6. Antibacterial Activity

The antibacterial activity of mixed oxides was carried out by exploring microdilution assays, the kill time curve, and the agar diffusion test against *S. aureus* (ATCC 25923).

The microdilution test in broth was performed for the evaluation of the minimum bactericidal concentration (MBC) of the solution [42], and it is described as follows: 100 µL aliquots of (Trypticase Soy Broth—TSB—Êxodo Científica, São Paulo, Brazil) were added to each microplate well (96 wells per microplate—Firstlab, Paraná, Brazil). Then, 100 µL of samples 0% Ag/TiO_2, 2% Ag/TiO_2, and 10% Ag/TiO_2, with initial concentrations of 100 mg/mL, was added to the first wells and, after homogenization, transferred to the second and so on, obtaining reductions of 1:2, 1:4, 1:8, 1:16, 1:32, 1:64, 1:128, and 1:256 relative to the initial concentration. Afterward, 10 µL aliquots of a bacterial suspension of *S. aureus* at 10^8 CFU/mL (0.5 turbidities on the McFarland scale) were added to the microplate wells, except for negative controls (wells with TSB broth without bacteria). The microplate was incubated at 37 °C for 24 h. After that, aliquots of the microplates were

seeded on the surface of the Plate Count Agar medium—PCA (Êxodo Científica, São Paulo, Brazil)—with the aid of a microplate replicator; then, the plate was again incubated at 37 °C for 24 h. All treatments were performed in triplicate.

For the kill time curve test, solutions of pure 0% Ag/TiO_2, 2% Ag/TiO_2, and 10% Ag/TiO_2 were used with concentrations of 4x MBC for each sample [42]. Reactors with 6.6 mL of the bacterial suspension of *S. aureus* at 10^8 CFU/mL (0.5 turbidities on the McFarland scale) received 3.3 mL of 0% Ag/TiO_2, 2% Ag/TiO_2, and 10% Ag/TiO_2 separately. A control reactor was prepared with 10 mL of bacterial suspension in 10^8 CFU/mL saline solution (0.5 in turbidity on the McFarland scale). Aliquots of 100 µL from the reactors were removed at fixed time intervals (1, 5, 10, 15, 30, 45, 60, 75, and 90 min) and dispersed in Petri dishes with a PCA agar medium. Colonies were counted and expressed as total viable counts (TVCs) after 24 h of incubation at 37 °C. This test was performed in triplicate.

The qualitative evaluation of the antibacterial activity of 0% Ag/TiO_2, 2% Ag/TiO_2, and 10% Ag/TiO_2 samples was performed using an agar diffusion test. In this test, the solutions were incorporated into 1 cm diameter disks of previously treated tilapia skin. As a control, tilapia skin was used without the incorporation of any antibacterial agents. After making the skin disks, a suspension of *S. aureus* (ATCC 25923) in saline solution (0.5 in turbidity on the McFarland scale) was prepared. With the aid of a swab, the bacterial suspension was seeded across the surface of the PCA agar medium. Then, tilapia skin disks with 0% Ag/TiO_2, 2% Ag/TiO_2, and 10% Ag/TiO_2 and pure skin (control) were aseptically deposited on the plates. The plates were incubated at 37 °C, and inhibition zones were measured after 24 h. The test was performed in triplicate.

2.7. Biofilm Formation and Counting Method

The biofilm formation inhibition activity was performed against the *S. aureus* strain (ATCC 25923) cultivated in a TSA medium (Tryptic Soy Agar), as reported in Ref. [41]. Colonies were transferred to 10 mL of saline solution, obtaining a bacterial suspension with a concentration of 10^8 CFU/mL (0.5 in turbidity on the McFarland scale). Then, 1 mL of this initial suspension was transferred to reactors with 9 mL of TSB broth (Trypticase Soy Broth), completing 10 mL of the solution at 10^7 CFU/mL. Tilapia skin disks with samples 0% Ag/TiO_2, 2% Ag/TiO_2, and 10% Ag/TiO_2 with concentrations of 4× MBC for each sample, and pure skin disks (control treatment) were added to the reactors and incubated at 37 °C for 24 h. After the incubation period, the disks were removed from the reactors, and 10 mL of saline solution was added. The resulting solutions were taken to an ultrasonic bath (f = 40 kHz) for 15 min to remove the species adhering to the walls of the reactors. Then, 100 µL aliquots were removed in triplicate from each system and plated on PCA. The error bars were calculated relative to the standard deviation of the three results.

3. Results and Discussion

3.1. Characterization

The morphology of the mixed oxides is characterized by the grains of both components (Ag and TiO_2), with sizes in the order of (305.02 ± 76.25) nm for 0% Ag/TiO_2—Figure 1a; (291.37 ± 62.83) nm for 2% Ag/TiO_2—Figure 1b; and (283.62 ± 109.05) nm for 10% Ag/TiO_2—Figure 1c. Overlaid EDX images for samples 0% Ag/TiO_2, 2% Ag/TiO_2, and 10% Ag/TiO_2 confirm the presence of elements Ti (red dots) and O (green dots)—Figure 1d—and Ti (green dots) and Ag (red dots) in Figure 1e,f for samples 2% Ag/TiO_2 and 10% Ag/TiO_2, respectively.

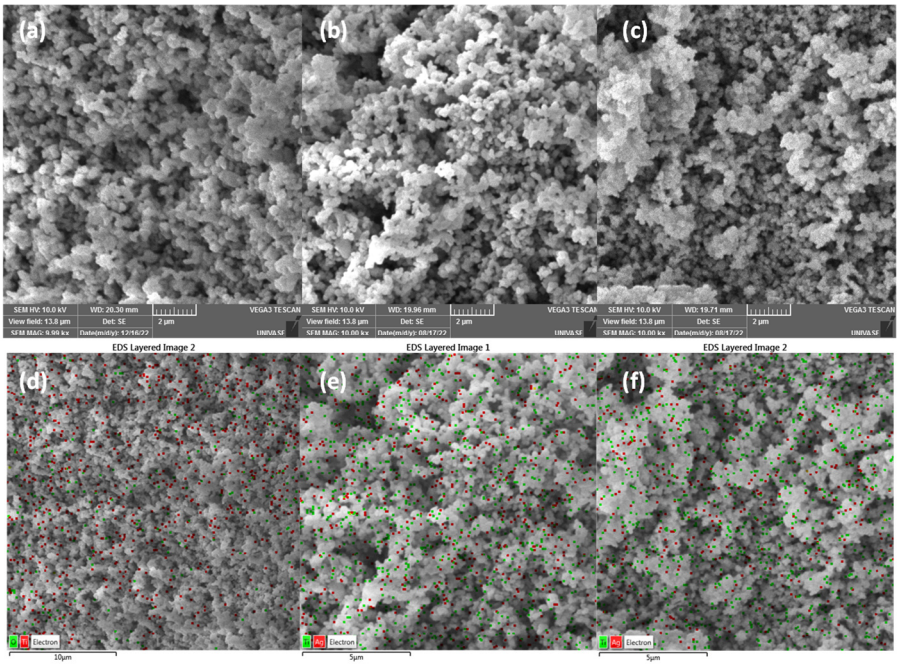

Figure 1. SEM images of (**a**) 0% Ag/TiO_2, (**b**) 2% Ag/TiO_2, and (**c**) 10% Ag/TiO_2 and overlaid EDX images of samples (**d**) 0% Ag/TiO_2 (Ti in red dots and O in green dots), (**e**) 2% Ag/TiO_2, and (**f**) 10% Ag/TiO_2 (Ti in green dots and Ag in red dots).

The FTIR spectrum of samples with increasing concentrations of silver in mixed oxides was evaluated within the range of 400–4500 cm^{-1} (see Figure 2a). The characteristic band of TiO_2 was identified at 671 cm^{-1}, which is assigned to the binding of oxygen and titanium (Ti-O-O) [43,44], and at 1638 cm^{-1} relative to the Ti-OH water folding modes [45,46], while the identified broadband at 3426 cm^{-1} is assigned to the stretching vibration of the OH group [46,47].

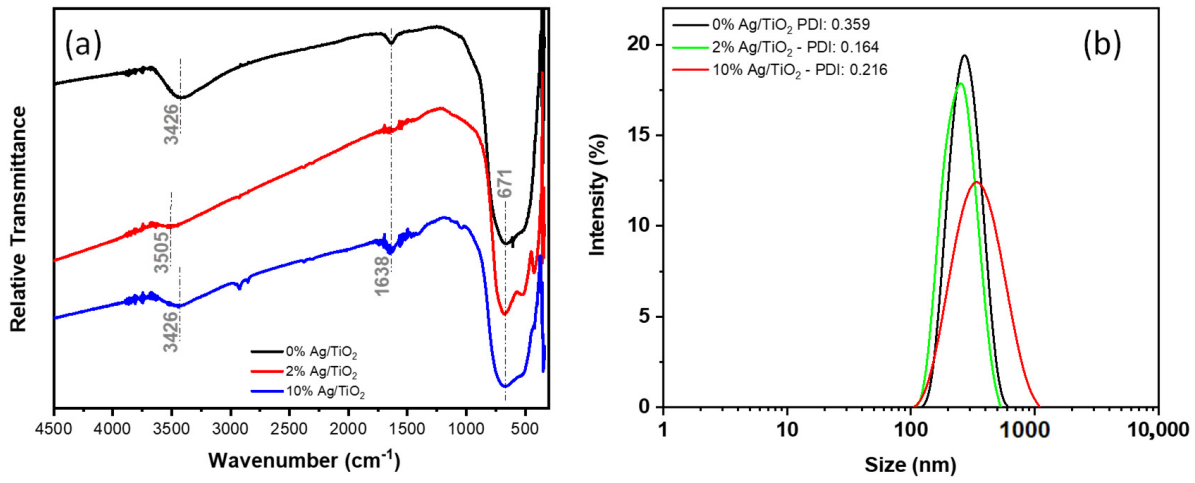

Figure 2. (**a**) FTIR spectrum of samples 0% Ag/TiO_2 (curve in black), 2% Ag/TiO_2 (curve in red), and 10% Ag/TiO_2 (curve in blue) and (**b**) hydrodynamic radius of dispersion of mixed oxides in water—0% Ag/TiO_2 (curve in black), 2% Ag/TiO_2 (curve in green), and 10% Ag/TiO_2 (curve in red).

The interaction between silver nanoparticles and titanium dioxide support can be identified from a new band at 1398 cm^{-1} as a response to the TiO_2-Ag bond [43,48,49].

The aggregation level of mixed oxide was evaluated from the measured distribution of the hydrodynamic radius of nanoparticles in water (see Figure 2b). As observed, the

aggregation level of grains confirms the structures in SEM images with a distribution of sizes centered in 274 nm for 0% Ag/TiO_2, 252 nm for 2% Ag/TiO_2, and 348 nm for sample 10% Ag/TiO_2.

In addition to the aggregation level and FTIR spectrum of the mixed oxide, the relevant information is obtained from the diffraction X-ray spectrum (Figure 3). According to the XRD analysis, all supports of TiO_2 (Figure 3a) are prevalent in the rutile crystal phase (88 to 98%) ICSD 01-075-1757, and the remaining part is the anatase crystal phase ICSD 01-071-1166. Mixed oxides (modified TiO_2 in the presence of precursor $AgNO_3$)—Figure 3b,c—confirmed the existence of peaks at 38.18° (111), 44.26° (200), 64.38° (220), and 77.33° (311), according to reference standard ICSD 01-087-0717 for the face-centered cubic crystal of silver, as reported by Kim et al. [50].

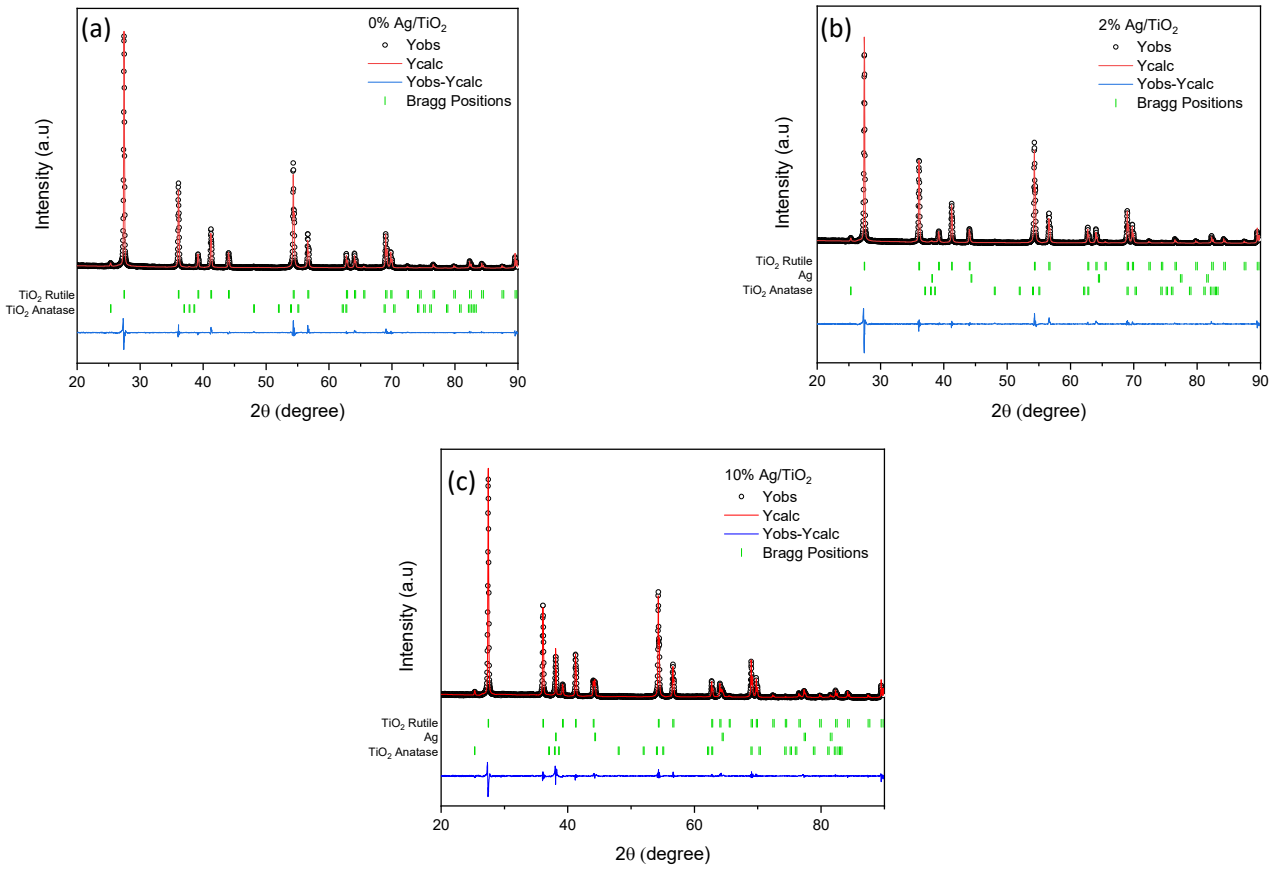

Figure 3. DRX spectrum for samples 0% Ag/TiO_2 (**a**), 2% Ag/TiO_2 (**b**), and 10% Ag/TiO_2 (**c**).

3.2. Antibacterial Assays

Minimal bactericidal concentration (MBC) assays were conducted for different experimental systems, as summarized in Figure 4a, confirming the presence of bacteria in the positive control column and the absence of contamination in the negative control column with different levels of critical concentrations for different compounds. As observed for columns in which samples were evaluated, negligible antibacterial activity was observed for sample 0% Ag/TiO_2 for an initial concentration of 10^8 CFU/mL. Under the progressive incorporation of silver nanoparticles in mixed oxides, it is possible to identify the MBC for samples 2% Ag/TiO_2 of 6.25 mg/mL and a reduction to 3.13 mg/mL as a response to the higher loading mass of silver in sample 10% Ag/TiO_2. These results confirm that silver introduces a relevant contribution to the overall antibacterial performance of the mixed oxide.

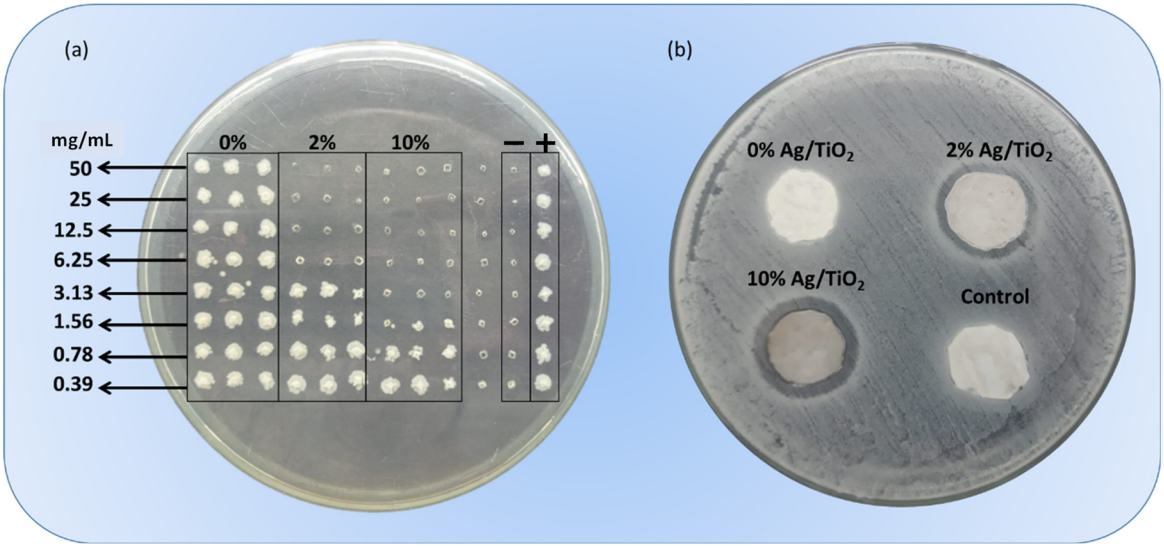

Figure 4. (**a**) MBC assays for different compounds at a progressive reduction in the concentrations against *S. aureus*. From left to right: positive control, negative control, 10% Ag/TiO_2, 2% Ag/TiO_2, and 0% Ag/TiO_2. (**b**) Inhibition zones for tilapia skin impregnated with mixed oxides: negative control, 10% Ag/TiO_2, 2% Ag/TiO_2, and 0% Ag/TiO_2.

The resulting inhibition halo assays for tilapia skin applied as a scaffold impregnated with mixed oxides are shown in Figure 4b. As can be seen, a negligible inhibition halo is observed for the negative control and in the absence of silver nanoparticles (samples control and 0% Ag/TiO_2). At an increasing concentration of silver in mixed oxides, an increasing inhibition halo is observed from images, (21.69 ± 0.43) mm for sample 2% Ag/TiO_2 and (23.81 ± 0.30) mm for sample 10% Ag/TiO_2, confirming the relevance of silver nanoparticles content on the overall antibacterial activity of the mixed oxide.

The kill time assays performed in the range of time from 5 min to 90 min for all samples are summarized in Figure 5. As expected, and as a consequence of the results from MBC and the inhibition halo, a negligible variation is observed for samples prepared in the absence of silver. Under the progressive incorporation of silver nanoparticles, the characteristic kill time is in an order of 45 min for the complete elimination of *S. aureus* for sample 2% Ag/TiO_2, while the increasing concentration of silver for values in the order of 10% Ag/TiO_2 reduces the time to 30 min, characterizing the most efficient activity of the mixed metal oxide at a higher content of silver.

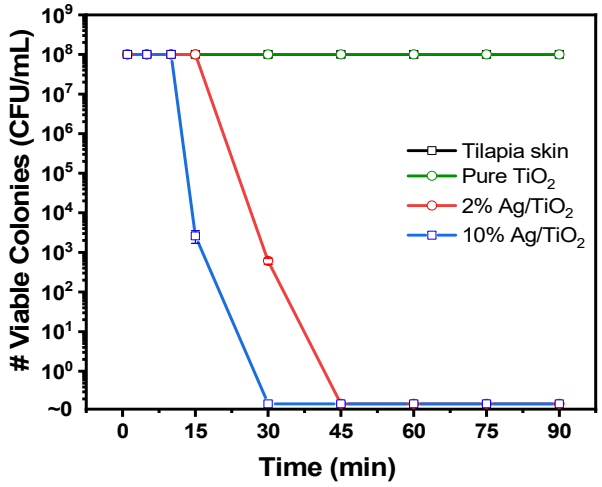

Figure 5. Kill time kinetics for tilapia skin impregnated with mixed oxides: negative control (curve in black), 10% Ag/TiO_2 (curve in blue), 2% Ag/TiO_2 (curve in red), and 0% Ag/TiO_2 (curve in green).

The inhibition of biofilm formation was evaluated by considering different antibacterial compounds measured from the relative variation in biofilm formation in tilapia skin and reactors by considering modified tilapia skin with mixed oxides used as an antibacterial surface. The results summarized in Figure 6 indicated that negligible antibiofilm activity was observed for all compositions—represented by the initial concentration (10^7CFU/mL) in the plot—with the exception of the tilapia skin impregnated with 10% Ag/TiO_2, reducing the amount of biofilm formation on both surfaces (skin and reactor) and confirming the potential of mixed oxides prepared at higher concentrations of silver in acting not only as a potential antibacterial agent but also as an antibiofilm component with the most important role assumed by silver nanoparticles as a concentration-dependent component against biofilm-forming *S. aureus*.

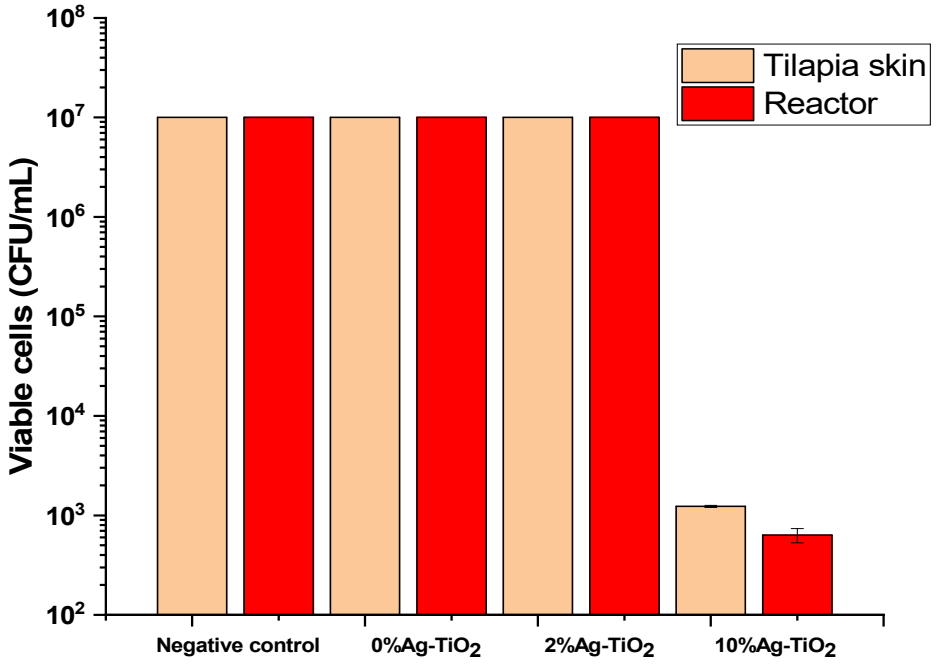

Figure 6. Biofilm inhibition evaluation for tilapia skin impregnated with mixed oxides: negative control, 10% Ag/TiO_2, 2% Ag/TiO_2, and 0% Ag/TiO_2.

4. Conclusions

The incorporation of mixed oxide (Ag/TiO_2) into tilapia skin provides additional antibacterial and antibiofilm activity relative to the intrinsic properties of the xenograft, characterizing this process as a low-cost and efficient method for the impregnation of oxides into xenograft. These results open possibilities that reduce the risk of contamination in burn treatments since antibiofilm activity is critical for the treatment. The incorporation of silver into TiO_2 is critical in the complete process since these nanoparticles are responsible for the attack of cells, the binding to sulfur proteins (interaction with thiol groups (-SH) and phosphorous components in DNA), and the inhibition of vital processes in bacteria and biofilms. The complete elimination of *S. aureus* from an initial concentration of 10^8 CFU/mL in 30 min is one of the most important results of this experimental system.

Author Contributions: Conceptualization, H.P.d.O. and L.M.S.C.; methodology, H.P.d.O., M.C.M., M.L.G., L.M.S.C. and M.M.d.C.; formal analysis, H.P.d.O. and L.M.S.C.; data curation, H.P.d.O. and J.A.A.F.; writing—original draft preparation, H.P.d.O.; writing—review and editing, M.C.M., M.L.G., J.A.A.F., L.M.S.C., M.M.d.C. and H.P.d.O.; supervision, H.P.d.O., L.M.S.C. and M.M.d.C.; project administration, H.P.d.O.; funding acquisition, H.P.d.O. All authors have read and agreed to the published version of the manuscript.

Funding: This work was supported by FACEPE, FINEP and CNPq. This study was financed in part by the Coordenação de Aperfeiçoamento de Pessoal de Nível Superior—Brasil (CAPES)—Finance Code 001.

Institutional Review Board Statement: Not applicable.

Informed Consent Statement: Not applicable.

Data Availability Statement: Data available on request due to restrictions.

Acknowledgments: Brazilian Funding Agencies FACEPE, FINEP, CAPES, and CNPq.

Conflicts of Interest: The authors declare no conflict of interest.

References

1. Loo, Y.Y.; Rukayadi, Y.; Nor-Khaizura, M.-A.; Kuan, C.H.; Chieng, B.W.; Nishibuchi, M.; Radu, S. In Vitro Antimicrobial Activity of Green Synthesized Silver Nanoparticles Against Selected Gram-negative Foodborne Pathogens. *Front. Microbiol.* **2018**, *9*, 1555. [CrossRef] [PubMed]
2. De Saravia, S.G.G.; Rastelli, S.E.; Angulo-Pineda, C.; Palza, H.; Viera, M.R. Anti-adhesion and antibacterial activity of silver nanoparticles and graphene oxide-silver nanoparticle composites. *Matéria* **2020**, *25*, e-12771. [CrossRef]
3. Rao, T.N.; Riyazuddin; Babji, P.; Ahmad, N.; Khan, R.A.; Hassan, I.; Shahzad, S.A.; Husain, F.M. Green synthesis and structural classification of Acacia nilotica mediated-silver doped titanium oxide (Ag/TiO_2) spherical nanoparticles: Assessment of its antimicrobial and anticancer activity. *Saudi J. Biol. Sci.* **2019**, *26*, 1385–1391. [CrossRef] [PubMed]
4. Deshmukh, S.P.; Mullani, S.B.; Koli, V.B.; Patil, S.M.; Kasabe, P.J.; Dandge, P.B.; Pawar, S.A.; Delekar, S.D. Ag Nanoparticles Connected to the Surface of TiO_2 Electrostatically for Antibacterial Photoinactivation Studies. *Photochem. Photobiol.* **2018**, *94*, 1249–1262. [CrossRef] [PubMed]
5. Lampé, I.; Beke, D.; Biri, S.; Csarnovics, I.; Csík, A.; Dombrádi, Z.; Hajdu, P.; Hegedűs, V.; Rácz, R.; Varga, I.; et al. Investigation of silver nanoparticles on titanium surface created by ion implantation technology. *Int. J. Nanomed.* **2019**, *14*, 4709–4721. [CrossRef]
6. Gudkov, S.V.; Serov, D.A.; Astashev, M.E.; Semenova, A.A.; Lisitsyn, A.B. Ag_2O Nanoparticles as a Candidate for Antimicrobial Compounds of the New Generation. *Pharmaceuticals* **2022**, *15*, 968. [CrossRef]
7. Rajabi, A.; Ghazali, M.J.; Mahmoudi, E.; Baghdadi, A.H.; Mohammad, A.W.; Mustafah, N.M.; Ohnmar, H.; Naicker, A.S. Synthesis, Characterization, and Antibacterial Activity of Ag_2O-Loaded Polyethylene Terephthalate Fabric via Ultrasonic Method. *Nanomaterials* **2019**, *9*, 450. [CrossRef]
8. Yin, I.X.; Zhang, J.; Zhao, I.S.; Mei, M.L.; Li, Q.; Chu, C.H. The Antibacterial Mechanism of Silver Nanoparticles and Its Application in Dentistry. *Int. J. Nanomed.* **2020**, *15*, 2555–2562. [CrossRef]
9. Ahmad, S.A.; Das, S.S.; Khatoon, A.; Ansari, M.T.; Afzal, M.; Hasnain, S.; Nayak, A.K. Bactericidal activity of silver nanoparticles: A mechanistic review. *Mater. Sci. Energy Technol.* **2020**, *3*, 756–769. [CrossRef]
10. Kanakaraju, D.; Kutiang, F.D.A.; Lim, Y.C.; Goh, P.S. Recent progress of Ag/TiO_2 photocatalyst for wastewater treatment: Doping, co-doping, and green materials functionalization. *Appl. Mater. Today* **2022**, *27*, 101500. [CrossRef]
11. Yerli-Soylu, N.; Akturk, A.; Kabak, Ö.; Erol-Taygun, M.; Karbancioglu-Guler, F.; Küçükbayrak, S. TiO_2 nanocomposite ceramics doped with silver nanoparticles for the photocatalytic degradation of methylene blue and antibacterial activity against Escherichia coli. *Eng. Sci. Technol. Int. J.* **2022**, *35*, 101175. [CrossRef]
12. Mariappan, A.; Pandi, P.; Rajeswarapalanichamy, R.; Neyvasagam, K.; Sureshkumar, S.; Gatasheh, M.K.; Hatamleh, A.A. Bandgap and visible-light-induced photocatalytic performance and dye degradation of silver doped HAp/TiO_2 nanocomposite by sol-gel method and its antimicrobial activity. *Environ. Res.* **2022**, *211*, 113079. [CrossRef]
13. Andre, R.D.S.; Zamperini, C.A.; Mima, E.G.D.O.; Longo, V.M.; Albuquerque, A.; Sambrano, J.R.; Machado, A.L.; Vergani, C.; Hernandes, A.C.; Varela, J.A.; et al. Antimicrobial activity of TiO_2:Ag nanocrystalline heterostructures: Experimental and theoretical insights. *Chem. Phys.* **2015**, *459*, 87–95. [CrossRef]
14. Nigussie, G.Y.; Tesfamariam, G.M.; Tegegne, B.M.; Weldemichel, Y.A.; Gebreab, T.W.; Gebrehiwot, D.G.; Gebremichel, G.E. Antibacterial Activity of Ag-Doped TiO_2 and Ag-Doped ZnO Nanoparticles. *Int. J. Photoenergy* **2018**, *2018*, 5927485. [CrossRef]
15. Dias, H.B.; Bernardi, M.I.B.; Bauab, T.M.; Hernandes, A.C.; Rastelli, A.N.D.S. Titanium dioxide and modified titanium dioxide by silver nanoparticles as an anti biofilm filler content for composite resins. *Dent. Mater.* **2018**, *35*, e36–e46. [CrossRef] [PubMed]
16. Chen, R.; Han, Z.; Huang, Z.; Karki, J.; Wang, C.; Zhu, B.; Zhang, X. Antibacterial activity, cytotoxicity and mechanical behavior of nano-enhanced denture base resin with different kinds of inorganic antibacterial agents. *Dent. Mater. J.* **2017**, *36*, 693–699. [CrossRef] [PubMed]
17. Li, S.; Zhu, Q.; Sun, Y.; Wang, L.; Lu, J.; Nie, Q.; Ma, Y.; Jing, W. Fabrication of Ag Nanosheet@TiO_2 Antibacterial Membranes for Inulin Purification. *Ind. Eng. Chem. Res.* **2020**, *59*, 7797–7804. [CrossRef]
18. Chambers, C.; Stewart, S.; Su, B.; Jenkinson, H.; Sandy, J.; Ireland, A. Silver doped titanium dioxide nanoparticles as antimicrobial additives to dental polymers. *Dent. Mater.* **2016**, *33*, e115–e123. [CrossRef]

19. Jiménez-Ramírez, A.J.; Martínez-Martínez, R.E.; Ayala-Herrera, J.L.; Zaragoza-Contreras, E.A.; Domínguez-Pérez, R.A.; Reyes-López, S.Y.; Donohue-Cornejo, A.; Cuevas-González, J.C.; Silva-Benítez, E.L.; Espinosa-Cristóbal, L.F. Antimicrobial Activity of Silver Nanoparticles against Clinical Biofilms from Patients with and without Dental Caries. *J. Nanomater.* **2021**, *2021*, 5587455. [CrossRef]
20. Gao, L.; Gan, W.; Xiao, S.; Zhan, X.; Li, J. A robust superhydrophobic antibacterial Ag–TiO_2 composite film immobilized on wood substrate for photodegradation of phenol under visible-light illumination. *Ceram. Int.* **2016**, *42*, 2170–2179. [CrossRef]
21. Uhm, S.-H.; Song, D.-H.; Kwon, J.-S.; Lee, S.-B.; Han, J.-G.; Kim, K.-N. Tailoring of antibacterial Ag nanostructures on TiO_2nanotube layers by magnetron sputtering. *J. Biomed. Mater. Res. Part B: Appl. Biomater.* **2013**, *102*, 592–603. [CrossRef] [PubMed]
22. Muflikhun, M.A.; Chua, A.Y.; Santos, G.N.C. Structures, Morphological Control, and Antibacterial Performance of Ag/TiO_2 Micro-Nanocomposite Materials. *Adv. Mater. Sci. Eng.* **2019**, *2019*, 9821535. [CrossRef]
23. Qais, F.A.; Shafiq, A.; Khan, H.M.; Husain, F.M.; Khan, R.A.; Alenazi, B.; Alsalme, A.; Ahmad, I. Antibacterial Effect of Silver Nanoparticles Synthesized Using *Murraya koenigii* (L.) against Multidrug-Resistant Pathogens. *Bioinorg. Chem. Appl.* **2019**, *2019*, 4649506. [CrossRef] [PubMed]
24. Durdu, S.; Aktug, S.L.; Korkmaz, K.; Yalcin, E.; Aktas, S. Fabrication, characterization and in vitro properties of silver-incorporated TiO_2 coatings on titanium by thermal evaporation and microarc oxidation. *Surf. Coatings Technol.* **2018**, *352*, 600–608. [CrossRef]
25. Thukkaram, M.; Cools, P.; Nikiforov, A.; Rigole, P.; Coenye, T.; Van Der Voort, P.; Du Laing, G.; Vercruysse, C.; Declercq, H.; Morent, R.; et al. Antibacterial activity of a porous silver doped TiO_2 coating on titanium substrates synthesized by plasma electrolytic oxidation. *Appl. Surf. Sci.* **2019**, *500*, 144235. [CrossRef]
26. Amjad, U.-E.; Lenzi, G.G.; Fernandes-Machado, N.R.C.; Specchia, S. MgO and Nb2O5 oxides used as supports for Ru-based catalysts for the methane steam reforming reaction. *Catal. Today* **2015**, *257*, 122–130. [CrossRef]
27. Colpini, L.M.S.; Lenzi, G.G.; Urio, M.B.; Kochepka, D.M.; Alves, H.J. Photodiscoloration of textile reactive dyes on Ni/TiO_2 prepared by the impregnation method: Effect of calcination temperature. *J. Environ. Chem. Eng.* **2014**, *2*, 2365–2371. [CrossRef]
28. Elshahawy, A.M.; Mahmoud, G.A.-E.; Mokhtar, D.M.; Ibrahim, A. The optimal concentration of silver nanoparticles in sterilizing fish skin grafts. *Sci. Rep.* **2022**, *12*, 19483. [CrossRef]
29. Ibrahim, A.; Soliman, M.; Kotb, S.; Ali, M.M. Evaluation of fish skin as a biological dressing for metacarpal wounds in donkeys. *BMC Veter-Res.* **2020**, *16*, 472. [CrossRef]
30. Guimarães, M.L.; da Silva, F.A.G.; da Costa, M.M.; de Oliveira, H.P. Coating of conducting polymer-silver nanoparticles for antibacterial protection of Nile tilapia skin xenografts. *Synth. Met.* **2022**, *287*, 117055. [CrossRef]
31. Júnior, E.M.L.; Filho, M.O.D.M.; Costa, B.A.; Alves, A.P.N.N.; De Moraes, M.E.A.; Uchôa, A.M.D.N.; Martins, C.B.; Bandeira, T.D.J.P.G.; Rodrigues, F.A.R.; Paier, C.R.K.; et al. Lyophilised tilapia skin as a xenograft for superficial partial thickness burns: A novel preparation and storage technique. *J. Wound Care* **2020**, *29*, 598–602. [CrossRef] [PubMed]
32. Tognetti, L.; Pianigiani, E.; Ierardi, F.; Mariotti, G.; Perotti, R.; Di Lonardo, A.; Rubegni, P.; Fimiani, M. Current insights into skin banking: Storage, preservation and clinical importance of skin allografts. *J. Biorepository Sci. Appl. Med.* **2017**, *5*, 41–56. [CrossRef]
33. Wang, T.; Yang, L.; Wang, G.; Han, L.; Chen, K.; Liu, P.; Xu, S.; Li, D.; Xie, Z.; Mo, X.; et al. Biocompatibility, hemostatic properties, and wound healing evaluation of tilapia skin collagen sponges. *J. Bioact. Compat. Polym.* **2020**, *36*, 44–58. [CrossRef]
34. Howaili, F.; Mashreghi, M.; Shahri, N.M.; Kompany, A.; Jalal, R. Development and evaluation of a novel beneficent antimicrobial bioscaffold based on animal waste-fish swim bladder (FSB) doped with silver nanoparticles. *Environ. Res.* **2020**, *188*, 109823. [CrossRef]
35. Bhat, V.; John, N.; Shetty, A.; Raj, V.; Joseph, S.; Kuriakose, R.; Hameed, S. Assessment of Flexural Strength and Cytotoxicity of Heat Cure Denture Base Resin Modified with Titanium Dioxide Nanoparticles: An In Vitro Study. *J. Contemp. Dent. Pr.* **2021**, *22*, 1025–1029. [CrossRef]
36. Neta, I.A.B.; Mota, M.F.; Lira, H.L.; Neves, G.A.; Menezes, R.R. Nanostructured titanium dioxide for use in bone implants: A short review. *Cerâmica* **2020**, *66*, 440–450. [CrossRef]
37. Guimarães, M.L.; da Silva, F.A.G.; de Souza, A.M.; da Costa, M.M.; de Oliveira, H.P. All-green wound dressing prototype based on Nile tilapia skin impregnated with silver nanoparticles reduced by essential oil. *Appl. Nanosci.* **2021**, *12*, 129–138. [CrossRef]
38. Ibrahim, A.; Hassan, D.; Kelany, N.; Kotb, S.; Soliman, M. Validation of Three Different Sterilization Methods of Tilapia Skin Dressing: Impact on Microbiological Enumeration and Collagen Content. *Front. Veter-Sci.* **2020**, *7*, 597751. [CrossRef]
39. Wijnhoven, S.W.; Peijnenburg, W.J.; Herberts, C.A.; Hagens, W.I.; Oomen, A.G.; Heugens, E.H.; Roszek, B.; Bisschops, J.; Gosens, I.; Van De Meent, D.; et al. Nano-silver—A review of available data and knowledge gaps in human and environmental risk assessment. *Nanotoxicology* **2009**, *3*, 109–138. [CrossRef]
40. Nie, Y.; Chen, J.; Xu, J.; Zhang, Y.; Yang, M.; Yang, L.; Wang, X.; Zhong, J. Vacuum freeze-drying of tilapia skin affects the properties of skin and extracted gelatins. *Food Chem.* **2021**, *374*, 131784. [CrossRef]
41. da Silva, F.A.G.; Eckhart, K.E.; da Costa, M.M.; Sydlik, S.A.; de Oliveira, H.P. Inhibition of biofilm formation induced by functional graphenic materials impregnated in Nile tilapia (Oreochromis niloticus) skin. *Appl. Surf. Sci.* **2022**, *576*, 151768. [CrossRef]
42. CLSI. *Performance Standards for Antimicrobial Susceptibility Testing*, 29th ed.; CLSI Supplement M100; Clinical and Laboratory Standards Institute: Wayne, PA, USA, 2019; p. 296.

43. Alsharaeh, E.H.; Bora, T.; Soliman, A.; Ahmed, F.; Bharath, G.; Ghoniem, M.G.; Abu-Salah, K.M.; Dutta, J. Sol-Gel-Assisted Microwave-Derived Synthesis of Anatase Ag/TiO_2/GO Nanohybrids toward Efficient Visible Light Phenol Degradation. *Catalysts* **2017**, *7*, 133. [CrossRef]
44. Safaei, M.; Taran, M. Optimal conditions for producing bactericidal sodium hyaluronate-TiO_2 bionanocomposite and its characterization. *Int. J. Biol. Macromol.* **2017**, *104*, 449–456. [CrossRef] [PubMed]
45. Chelli, V.R.; Chakraborty, S.; Golder, A.K. Ag-doping on TiO_2 using plant-based glycosidic compounds for high photonic efficiency degradative oxidation under visible light. *J. Mol. Liq.* **2018**, *271*, 380–388. [CrossRef]
46. León, A.; Reuquen, P.; Garín, C.; Segura, R.; Vargas, P.; Zapata, P.; Orihuela, P.A. FTIR and Raman Characterization of TiO_2 Nanoparticles Coated with Polyethylene Glycol as Carrier for 2-Methoxyestradiol. *Appl. Sci.* **2017**, *7*, 49. [CrossRef]
47. Yang, C.; Zhang, H.; Gu, W.; Chen, C. Preparation and mechanism investigation of highly sensitive humidity sensor based on Ag/TiO_2. *Curr. Appl. Phys.* **2022**, *43*, 57–65. [CrossRef]
48. Desiati, R.D.; Taspika, M.; Sugiarti, E. Effect of calcination temperature on the antibacterial activity of TiO_2/Ag nanocomposite. *Mater. Res. Express* **2019**, *6*, 095059. [CrossRef]
49. Ganapathy, M.; Senthilkumar, N.; Vimalan, M.; Jeysekaran, R.; Potheher, I.V. Studies on optical and electrical properties of green synthesized TiO_2@Ag core-shell nanocomposite material. *Mater. Res. Express* **2018**, *5*, 045020. [CrossRef]
50. Kim, Y.E.; Kim, B.; Lee, W.; Na Ko, Y.; Youn, M.H.; Jeong, S.K.; Park, K.T.; Oh, J. Highly tunable syngas production by electrocatalytic reduction of CO_2 using Ag/TiO_2 catalysts. *Chem. Eng. J.* **2020**, *413*, 127448. [CrossRef]